

**Best  
Available  
Copy**

12  
B.S.

**LEVEL III**

ADA082615

**Semiannual Technical Summary**

**DTIC**  
**ELECTE**  
**S** **D**  
APR 3 1980

**Seismic Discrimination**

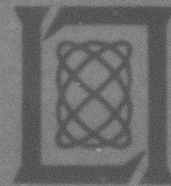
30 September 1979

Prepared for the Defense Advanced Research Projects Agency  
under Electronic Systems Division Contract F19628-78-C-0002 by

**Lincoln Laboratory**

MASSACHUSETTS INSTITUTE OF TECHNOLOGY

LEXINGTON, MASSACHUSETTS



Approved for public release; distribution unlimited.

80 3 31 070

FILE COPY

The work reported in this document was performed at Lincoln Laboratory, a center for research operated by Massachusetts Institute of Technology. This research is a part of Project Vela Uniform, which is sponsored by the Defense Advanced Research Projects Agency under Air Force Contract F19628-78-C-0002 (ARPA Order 512).

This report may be reproduced to satisfy needs of U.S. Government agencies.

The views and conclusions contained in this document are those of the contractor and should not be interpreted as necessarily representing the official policies, either expressed or implied, of the United States Government.

This technical report has been reviewed and is approved for publication.

FOR THE COMMANDER

*Raymond L. Loiselle*

Raymond L. Loiselle, Lt. Col., USAF  
Chief, ESD Lincoln Laboratory Project Office

Non-Lincoln Recipients

**PLEASE DO NOT RETURN**

Permission is given to destroy this document  
when it is no longer needed.

(12)

MASSACHUSETTS INSTITUTE OF TECHNOLOGY

LINCOLN LABORATORY

SEISMIC DISCRIMINATION

DTIC  
ELECTE  
APR 3 1980  
S D  
C

SEMIANNUAL TECHNICAL SUMMARY REPORT  
TO THE  
DEFENSE ADVANCED RESEARCH PROJECTS AGENCY

*Approved*

1 APRIL - 30 SEPTEMBER 1979

ISSUED 8 FEBRUARY 1980

Approved for public release; distribution unlimited.

LEXINGTON

MASSACHUSETTS

# ABSTRACT

Lincoln Laboratory is continuing the task of carrying out the design and specification of a Seismic Data Center which will fulfill U.S. obligations that may be incurred under a possible future Comprehensive Test Ban Treaty. This report includes 9 contributions, summarizing progress in the Data Center design and associated seismic research. These contributions are grouped as follows: Seismic Data Center (3 studies), analysis of Seismic Research Observatory data (3 studies), and general seismology (3 studies). An update to the Publications List is included.

Accession For	
NTIS GMAH	<input checked="" type="checkbox"/>
DOC TAB	
Unannounced Justification	
By _____	
Distribution/ _____	
Availability Codes	
Dist A	Avail and/or special



## CONTENTS

Abstract	iii
Summary	vii
 I. SEISMIC DATA CENTER	 1
A. Seismic Data Center Design	1
1. Data-Base Subsystems	1
2. Seismic Analysis Station	2
3. Intercomputer Communication Subsystem	2
B. Development of Interim Systems	2
1. Data Storage and Access Methods	3
2. User Interaction	3
3. Event Association and Location Processing	4
C. Automation of Analyst Functions	4
1. Picking Signal Onset Times	4
2. Magnitude Measurements	5
3. Complexity and Spectral Ratio	6
 II. ANALYSIS OF SRO DATA	 9
A. Detection Capability of the SRO/ASRO Network	9
B. Discrimination Performance of the SRO/ASRO Network	10
C. The Limited Research Value of the SRO Long-Period Records	12
 III. GENERAL SEISMOLOGY	 23
A. Spectra of Crustal Phases Recorded Digitally in Eastern Canada	23
B. More Moment Tensor Estimation from Long-Period Body Waves	23
C. Synthetic Seismograms for Explosive Sources	24
 IV. PUBLICATIONS LIST	 33
 Glossary	 35

PRECEDING PAGE NOT FILMED  
BLANK

## SUMMARY

This is the thirty-first Semiannual Technical Summary (SATS) report describing the activities of Lincoln Laboratory funded under Project Vela Uniform. This report covers the period 1 April to 30 September 1979. Project Vela is a program of research into the discrimination between earthquakes and nuclear explosions by seismic means. The current emphasis of the project is in the development of the data-handling and analysis techniques that might be appropriate for the monitoring of a potential Comprehensive Test Ban Treaty, presently under negotiation. The Lincoln Laboratory program during FY 79 has had two objectives. The first is to carry out a detailed design study, and produce hardware and software specifications for a Seismic Data Center (SDC) which will fulfill U.S. obligations that may be incurred under the Comprehensive Test Ban Treaty, and under any international agreement that may be associated with this treaty. The second is to carry out seismic research, with particular emphasis on those areas directly related to the operations of the SDC.

The preliminary design stages for the SDC have now been completed. A 264-page document detailing the objectives, requirements, and design philosophy of such a Center has been completed and submitted as a special internal report to the Nuclear Monitoring Research Office of the Defense Advanced Research Projects Agency. In Sec. I of this SATS, we outline a basic overview of the SDC design and describe progress in the development of an interim system which will carry out a limited number of the objectives of the final version of the proposed Center. We also describe progress being made in the automation of some functions such as magnitude determination to assist analyst operations.

We are continuing our analysis of data produced by the network of Seismic Research Observatories (SROs), the installation of which is nearing completion. The network currently consists of 17 digitally recording stations and now provides fairly good global capability for detection, discrimination, and source mechanism determination. Three studies using SRO data are described in Sec. II. The actual network detection capability of the network of 12 stations operating during January to July 1978 has been determined and shown to fall only slightly short of that predicted from individual station detection characteristics. A discrimination experiment for Eurasian events shows network complexity averages to be a surprisingly good discriminant. It is shown that the current response characteristics of the long-period SRO data channels severely limit the network's capability to carry out the simplest method of source mechanism determination, that of fault-plane solutions.

Section III contains three studies in the field of general seismology. We are continuing our interest in regional seismology and have attempted to quantify the apparent anelastic properties of the lithosphere in eastern North America using data from the Eastern Canada Telemetered Network. The ratio of shear-to-compressional attenuation is shown to be close to unity from spectra of local events, compared with approximately four from teleseismic signals. Previously described attempts to estimate the moment tensor from long-period body waves have been developed further, and double-couple components of this tensor between 71 and 85 percent obtained for three events in greatly different seismic regions. A method for constructing synthetic seismograms when only the amplitude spectrum of the reduced velocity potential is known is applied to the Salmon nuclear explosion using the assumption of minimum phase.

An update to the Publications List of the Applied Seismology Group printed in the 31 March 1977 SATS is included as Sec. IV.

M. A. Chinnery

## SEISMIC DISCRIMINATION

### I. SEISMIC DATA CENTER

#### A. SEISMIC DATA CENTER DESIGN

During the period covered by this SATS, the major part of Lincoln Laboratory's program in Seismic Discrimination has been devoted to the formulation of a design for a Seismic Data Center (SDC), which could assume U.S. seismic-data-management responsibilities in the event that international agreement is reached on a Comprehensive Test Ban Treaty. This design is described in a Special DARPA Report dated 30 September 1979. Here, we briefly summarize the contents of that report.

First, the report details the specific requirements which determined the design. These requirements are based on our current estimate of the needs to monitor a Comprehensive Test Ban Treaty using National Seismic Stations delivering data from numerous participants in an International Seismic Data Exchange. Since the actual requirements, in some particulars, will be determined by ongoing negotiations, the design requirements were deliberately chosen to be conservative. The flexibility and expansibility of the basic architectural approach ensure that the Seismic Data Management System (SDMS) will meet all the treaty requirements.

Next, the DARPA report outlines the basic computer architecture of the SDC, which is a multiple computer distributed system. This architecture was chosen to allow flexible growth of the system with reliable operation in handling the large amounts of data planned for the operational system. A set of subsystems are identified, and these are shown schematically in Fig. I-1. The report includes detailed discussions of the operational procedures and data flows within the SDC, and then gives a detailed discussion of the top-level design of each of the major subsystems. The configuration of the key subsystems is discussed in somewhat more detail below.

##### 1. Data-Base Subsystems

The reliable, responsive handling of the large quantities of waveform data and the associated parameter data is a major concern of the SDMS. The approach is to implement multiple modules which can control large disks, high-density tapes, or combinations of these peripherals. The requirements for these modules are the ability to handle large amounts of data on multiple peripherals with high reliability. The chosen approach for these modules is to use a pair of small mini-computers, each with a dual-access controller with two strings of peripherals. By this organization, a failure of any component in the module except the physical storage media will not render inaccessible any of the data under control of the module.

The basic approach to storing the waveform and parameter data has been worked out and is documented in the design report. The waveform data will be stored on disk in 2-kbyte blocks with an index structure which allows the rapid retrieval of data by time interval. The data will be stored on disk as they are received by the system over the communication link from the DoE computer system. Within a few hours after they are received, the data will be written on a tape which will collect all the data from a specific 2-hr period of occurrence. The data will remain on the disk and hence be quickly accessible until the disk space is needed to hold newly arriving data. After the data are overwritten on the disk, they will be accessible by mounting the tape



containing the appropriate time interval. This will allow data from any arbitrary time to be retrieved within a few minutes.

The parameter data base will also use the reliable storage module hardware configuration, but will use the UNIX operating system instead of a special operating system needed to facilitate handling the large amounts of data by the waveform data-base modules.

## 2. Seismic Analysis Station

The principal user interface with the SDC will be through a pair of high-quality display screens supported on a dedicated computer connected to the rest of the SDMS by the intercomputer communication subsystem. The two displays will be used, a 132-column alphanumeric display and keyboard for display of and interaction with parameter data and a high-resolution refreshed graphics display and manual input device such as a data tablet for display of and interaction with the waveform data. These displays will be supported by a dedicated computer with disk and tape storage. This computer will use the UNIX operating system to provide an interactive capability to support seismic analysis. Software used at this analysis station will be developments and improvements of software currently used for research at Lincoln Laboratory.

## 3. Intercomputer Communication Subsystem

The central element in the distributed architecture chosen for the SDC is the intercomputer communication subsystem, which will consist of a local computer network using a contention packet protocol to share a common passive communication medium. The top level of this design is presented in the DARPA report and the set of open issues to be resolved in completing the design are presented in an appendix. The investigation of the design details and the procurement of the commercially available components are progressing. The design of the detailed communication protocols and the software to implement the intercomputer communication subsystem are being pursued.

A. G. Gann  
M. A. Chinnery

## B. DEVELOPMENT OF INTERIM SYSTEMS

As part of our work on the SDC, we have started to design an interim system called Mod I. Initially, the system will run on the Applied Seismology Group's current PDP-11/50 computer and its function will be to produce a seismic bulletin by working with parameter data only (i.e., waveform data will not be considered). Later, expanded versions of Mod I will utilize a PDP-11/70, which is under procurement.

There are two reasons for implementing the Mod I system. The first is to provide a test bed for trying out various algorithms, user interfaces, etc., that are being considered for use in the final SDC system. For this purpose, we intend to use a variety of data sets, including data collected during the International Seismic Month and analyzed at Lincoln Laboratory,<sup>†</sup> and data from the International Seismological Center (ISC) and elsewhere. Previous analyses of these data will provide us with a benchmark against which to measure the results of various algorithms.

The second use of Mod I will transpire if the recommendations of the Conference of the Committee on Disarmament are realized. In their report CCD/558 dated 8 March 1978, the

<sup>†</sup> R. T. Lacoss, R. E. Needham, and B. R. Julian, "International Seismic Month Event List," Technical Note 1974-14, Lincoln Laboratory, M.I.T. (27 February 1974), DDC AD-776021/8.

Committee proposed an International Seismic Data Exchange using the World Meteorological Organization's Global Telecommunication System (WMO/GTS). Should this agreement materialize, or if any preliminary experiments related to this data exchange are carried out, the Mod I system will be used for data analysis and bulletin preparation.

The design of the Mod I system will involve three areas that are relevant to the SDMS design, namely:

- (1) Data Storage and Access Methods
- (2) User Interaction
- (3) Event Association and Location Processing

The rest of this section will discuss these areas.

#### 1. Data Storage and Access Methods

In the final SDC, the main event/arrival lists will be stored on the Parameter Data Base Subsystem. Users of the General Services Computer and the Seismic Analysis Stations will request time-interval portions of the list to be moved to a local working data base, modified, and later returned to the main data base.

This division between the main data base and the working data base has been carried over to the Mod I design. As described, the main data base will be accessed infrequently and the retrievals will be specified in terms of a time interval. Therefore, the main data base will be organized sequentially in time order, and retrievals will be handled by a simple scan or by a binary search for the start time.

The working data base, on the other hand, must be quickly accessible by both time and record ID. Therefore, we will probably want to construct indexes into the working data base for both of these parameters. The complexity of these indexes can vary according to the speed required to provide sufficient response in an interactive system. Thus, Mod I will provide a convenient means to determine how complex an implementation method will be required.

In regard to the actual data representation, we have designed a flexible format to be used in implementing Mod I that may be carried over to the final SDMS if it proves satisfactory. First, the data will be stored in a binary rather than an alphanumeric format. The binary format will require less space and conversion time than alphanumeric format, and will make it easier to implement a general file access system. Second, each file will contain within its header a list of the parameters that make up the records of that file. It has been our experience with other seismic software that it is impossible to predict in advance exactly which parameters will be required for a fully functioning system, so a flexible record format will allow us to add or remove parameters as the system's needs change. The implementation we have designed is such that programs will work (without recompilation) on any file format that contains a superset of the parameters used by that program.

#### 2. User Interaction

The complete details of the user interaction with the Mod I system have not yet been specified. In fact, one of the purposes of Mod I is to give us an environment where various approaches may be tried out with an actual analyst to see which of them is the most productive. "Human engineering" is not a well-defined field; yet, for the analysts to achieve maximum productivity, it is essential that they have the tools that are best fitted to their needs.

Although we have not specified the exact details of the interactions, we do know what functions need to be carried out in the most minimal system, and will begin by providing at least one method of carrying out each of these functions. The user must be able to display the arrival and event data in various formats: the raw lists, selected parameters and selected list items, or a merged list giving an event and its associated arrivals. He must be able to easily modify certain parameter values (such as phase) and to change the associations of arrivals with events. He must be able to invoke seismic programs to compute locations, residuals, etc. And he should be able to enter a "trial" mode wherein none of his tentative results are made a permanent part of the data base until he chooses to accept or reject them.

### 3. Event Association and Location Processing

The general association problem is a fairly complicated one which can lead to combinatorial explosion. For example, if there are  $n$  arrivals from  $k$  events, then there are on the order of  $2^{nk}$  combinations of arrivals to be examined in order to find the proper associations. Because of this, a number of heuristics are used to reduce the search space to a manageable size.

The NEIS, ISC, and AFTAC use automatic association algorithms. Although the current version of the NEIS algorithm identifies about 80 percent of the events correctly, there is still a great deal of research to be done on the association problem.

Rather than provide a single association algorithm, we plan to provide a number of association tools which will aid an analyst in the interactive association task. Each tool is simpler to implement than a complete association algorithm would be, and thus it will become available to analysts sooner. Additional tools will be developed in response to analysts' needs. Each analyst will be able to combine the automatic tools in the way which fits most comfortably with his own style. Ultimately, much of the association process will be accomplished automatically by the appropriate combination of tools.

L. J. Turek  
K. R. Anderson

## C. AUTOMATION OF ANALYST FUNCTIONS

The extremely large data volumes anticipated as input to the SDC will require substantial participation by seismic analysts in reviewing detections and measuring simple waveform parameters such as signal onset times, magnitudes, and discriminants such as complexity and spectral ratio. We are currently investigating the extent to which these analyst functions can be automated, and it appears that making the measurements associated with magnitude determination, at least, can be carried out with a fair degree of success. None of the automated procedures are intended to replace analysts, but considerable savings in time can be realized even from partial success in such methods so that the analyst's function is mainly one of reviewing and correcting, where necessary, unavoidable erroneous measurements. We are currently studying the following problems.

### 1. Picking Signal Onset Times

Although even an inexperienced analyst can rapidly and correctly identify the onset of a signal, this appears to be surprisingly difficult to automate except in cases where the dominant frequencies of signal and noise are radically different, when simple gradient techniques are useful. We have been studying the application of prediction-error filters, both adaptive and non-adaptive, which ideally will suppress the noise and spike the seismogram at the onset time.

In practice, our experience to date is that such techniques effectively high-pass filter the data since the most predictable feature of the noise is its longer period character. Some degree of signal spiking is observed, generally near the signal onset time, but the accuracy is so poor that substantial analyst correction would be necessary for virtually all time picks made. Predictive deconvolution is thus apparently more useful as a detector than as an indicator of signal onset time.

## 2. Magnitude Measurements

Both body-wave magnitude  $m_b$  and surface-wave magnitude  $M_s$  require only simple measurements of amplitude  $A$  and period  $T$  from the seismogram. In the case of  $m_b$ ,  $A$  and  $T$  are simply the maximum peak-to-peak amplitude and corresponding period within the first five cycles of the short-period P-wave. For  $M_s$ ,  $A$  is the maximum trace amplitude within the surface-wave train of  $18 < T < 22$  sec. Both are readily automated, and we have written simple algorithms which successfully reproduce analyst measurements of these parameters, as follows.

### a. $m_b$

Once the onset time has been picked, a time window starting 4 sec before and ending 16 sec after the arrival time is extracted from the data. This window is then phase-free bandpass-filtered with 6-dB points at 0.4 and 2.5 Hz. (The window is longer than strictly necessary so that filter end effects can be avoided.) Starting at the onset time, the first 10 zero crossings are determined, and this defines the initial 5 cycles of the waveform. The largest trace amplitude within these 5 cycles is obtained, together with its closest maximum or minimum (if the largest trace amplitude is a minimum, or vice versa). The times at which these are measured are then stored as markers, and the required values of  $A$  and  $T$  are retrieved from the original seismogram as the difference in amplitude and twice the difference in time. Figure I-2 shows the markers determined by this technique for a set of 8 SRO short-period detections for an event of PDE Bulletin  $m_b = 5.4$ . On each seismogram are shown markers corresponding to the analyst time pick (P) and markers A and B chosen by the algorithm as points from which amplitude and period are to be measured. It can be seen that, in each case, the points picked are similar to those which would be made by an analyst. This algorithm was extensively used in the SRO discrimination study described in Sec. II-B, and agreed with picks which would be made by the author as an analyst for more than 95 percent of the waveforms studied, considerably reducing the time taken on making these manually.

### b. $M_s$

Since long-period data contribute little, if at all, to epicenter location, this is best carried out after event location is determined. For each long-period seismogram, a time window corresponding to group velocities  $2.5 < U < 3.5$  is retrieved, and the horizontal components converted to radial and transverse by rotation into the station-epicenter azimuth. Each seismogram is then phase-free bandpass-filtered with 6-dB points at 0.0625 and 0.0417 Hz (16- to 24-sec period). The time at which this filtered waveform is maximum is then stored as a marker and displayed on the original data. Figure I-3 shows the markers determined by this method for 9 long-period vertical seismograms windowed for Rayleigh waves from a presumed nuclear explosion in Western Kazakh, USSR. The points picked at stations GUMO and NWA0 are somewhat dubious, and would almost certainly be rejected by an analyst; the other 7 are satisfactory. This technique

has been applied to several-hundred waveforms in the course of the discrimination study mentioned above, and agreed with measurements which would be made by an analyst with about 70-percent success. When the 20-sec signal-to-noise ratio exceeded 2, and there were no interfering events, it was generally successful. The markers obtained must be displayed together with the original data so that the dispersive character of surface-wave trains can be employed by the analyst as a diagnostic of a true arrival. The analyst intervention consists more of rejecting dubious measurements rather than correcting erroneous ones. Obvious sophistications which could be applied to this technique include the use of either polarization filtering, or the determination of epicenter azimuth from the unrotated data, to confirm that the waveform is associated with the event being studied. In addition, narrower group-velocity windows can be used if calibration of dispersion over the surface of the globe is made. All of these methods are currently being investigated.

### 3. Complexity and Spectral Ratio

Once a time pick has been made, these are readily determined since they have simple and unambiguous definitions. In certain cases (e.g., close events with large amounts of high frequency, or substantial inherent complexity due to either regions of triplication in the travel-time curves or clear depth phases), it may not be desired to measure these parameters from certain waveforms.

In conclusion, with the exception of picking onset times, automatic algorithms can be a considerable aid to the analyst in measuring waveform parameters.

R. G. North

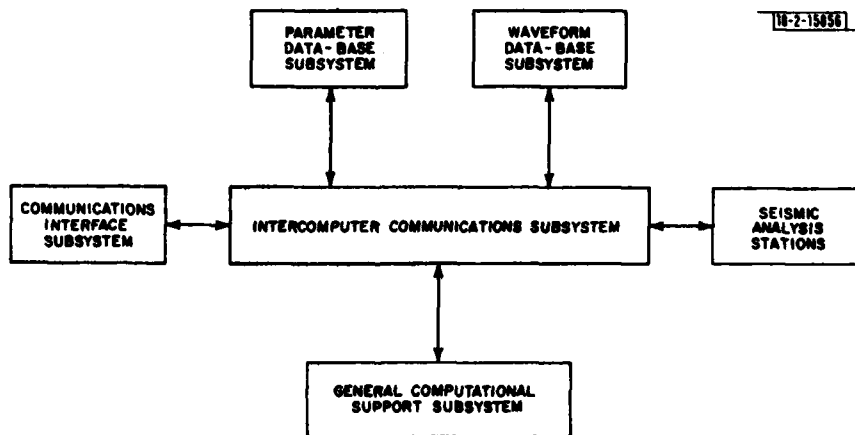


Fig. I-4. SDC computer system architecture.



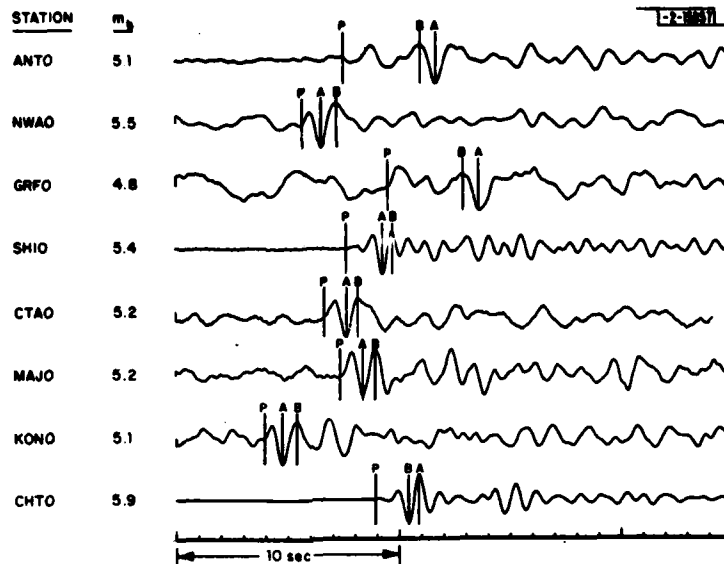


Fig. I-2. Eight short-period seismograms from an event in Iran of PDE Bulletin  $m_b = 5.4$  (7 December 1978). On each are shown analyst-selected P-wave arrival time, and points chosen by algorithm described in text to be those from which  $m_b$  is determined (markers A and B). Resulting values of  $m_b$  are given at left of each seismogram.

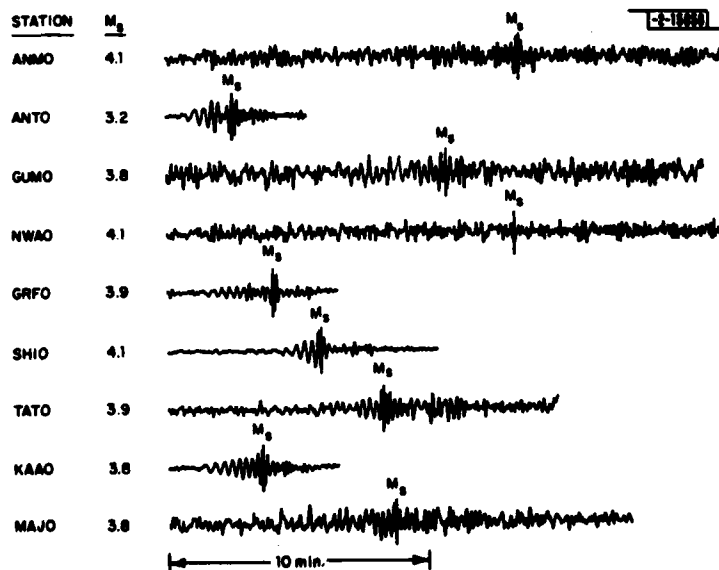


Fig. I-3. Nine long-period vertical group-velocity windows corresponding to an event in Western Kazakh (17 October 1978). Automatic determinations of peak 20-sec amplitude are shown by markers " $M_s$ ," and resulting  $M_s$  values are given to left of each seismogram. Markers for GUMO and NWAQ would probably be rejected by an analyst.

## II. ANALYSIS OF SRO DATA

### A. DETECTION CAPABILITY OF THE SRO/ASRO NETWORK

Several authors<sup>1,2</sup> have measured the detection characteristics of individual stations of the SRO/ASRO network. We present here an evaluation of the network detection capability of all the stations. There are now 17 stations currently operating, and the coverage of global seismicity that they provide should result in fairly good network detection characteristics. We have not yet received any data from the most recently installed station (BCAO-Bangui) but have large amounts of data produced by the remaining 16 stations. In August and September 1978, four stations in Eurasia-SHIO (Shillong, India), ANTO (Ankara, Turkey), GRFO (Graefenberg, Germany), and KONO (Kongsberg, Norway) started producing data, and we now have 5 to 6 months of detections from each.

Unfortunately, no bulletin exists for this period, the SDAC Bulletin having skipped the interval from August 1978 through March 1979, and the only usable form of the NEIS Bulletin, the monthly summaries, being at this date complete only up to May 1978. This lack of bulletin information precludes the use of these 4 new stations in the measurement of network detection capability. Had we been able to include these, the network statistics would have been considerably improved, particularly for Eurasia. This lack of event bulletins has continually hampered our usage and analysis of the SRO data.

We have selected the time interval January through July 1978 for this analysis. The event bulletin used was that produced by SDAC and was retrieved from the datacomputer. For each of the 12 stations used, we have determined station detection characteristics for all events with 100° distance. The results obtained for each were essentially similar to those calculated previously;<sup>2</sup> the only new station studied was BOCO (Bogota, Columbia). We have also determined the network detection characteristics for all events globally, and separately (since the stations are concentrated in that region, and we would thus expect better performance) for Eurasia, here simply defined as the northern half of the eastern hemisphere. Figures II-1 and II-2 show the detection performance (detection by at least one station of the network) for all events in Eurasia and the world, respectively. As expected, detection is better for Eurasia (994 of 1253 events, or 79 percent, detected) than for the entire world (1986 of 2616, or 76 percent). At  $m_b = 4.0$ , detection probabilities were 0.696 for Eurasia and 0.609 for the entire world.

Simulations of network detection capabilities are generally based upon the joint probability of detection given individual station detection characteristics. The latter are estimated from background-noise levels and other factors such as station magnitude bias and amplitude-distance relations. Such simulations necessarily involve complicated statistical analysis, and the number of input variables and their associated errors are large. Since we have determined both individual station and entire network capability, we may test here the final stage in such calculations - that of estimating network characteristics from those of the separate stations.

The probability of detection  $P_1^N$  at at least one of  $N$  stations, given the probability  $P_i$  at each station, is given by

$$1 - P_1^N = \prod_{i=1}^N (1 - P_i) \quad .$$

Figures II-3 and II-4 show the resulting estimates of network detection capability for Eurasia and the world, respectively. These may be compared with the actual performances given in Figs. II-1 and II-2. Actual and predicted capabilities at several magnitudes are given in Table II-1.

TABLE II-1 ACTUAL AND PREDICTED DETECTION PROBABILITIES AT VARIOUS MAGNITUDES FOR EURASIA AND THE WORLD				
Magnitude ( $m_b$ )	Eurasia		World	
	Actual	Predicted	Actual	Predicted
3.5	0.619	0.650	0.633	0.780
4.0	0.696	0.750	0.609	0.778
4.5	0.879	0.923	0.847	0.966
5.0	0.960	0.998	0.962	1.000

This table indicates that actual network detection performance is in all cases less than predicted, the discrepancy being smaller for Eurasian events. We have, of course, determined individual station capability only for events within  $100^\circ$ , and this may somewhat bias the results. Nevertheless, although it falls short of prediction, the detection capability of the SRO/ASRO network is quite respectable considering the shortcomings of automatic detectors. Eurasian capability should be considerably improved by the addition of stations ANTO, SHIO, GRFO, and KONO, and should a bulletin ever appear for the time interval over which they have operated, we shall re-evaluate network performance at that time.

In the context of input data rates and handling requirements for the SDC currently being designed by this group, the following numbers may be of interest. By assuming detection out to  $100^\circ$  distance, perfect performance (i.e., every station within range detecting) should have produced 22,258 possible detections from the 2,616 events during the time interval studied — the total number associated with an event in the bulletin. At the current rate of performance of the detector installed at the SRO/ASRO stations, the number of detections made was very close to that expected if the detectors were perfect, even though only ~20 percent were associated.

R. G. North

#### B. DISCRIMINATION PERFORMANCE OF THE SRO/ASRO NETWORK

Of the 17 SRO/ASRO stations installed, 9 are located in Eurasia. Therefore, good azimuthal and distance coverage is provided for Eurasian events, and we describe here the results of a discrimination experiment using  $M_s$  (both Rayleigh and Love) vs  $m_b$ , and complexity and spectral ratio determined solely from the 9 Eurasian stations. In order to use the most recently installed stations, we have studied events in the time interval July through December 1978. All events in the NEIS Preliminary Bulletin within the land mass of Eurasia (excluding Kamchatka, Kuril, Japan, and offshore islands) were laboriously typed in to form a database of 90 events for this study.

Of these events, 56 were shallow earthquakes (depth < 70 km), 14 intermediate-depth (70- to 225-km) earthquakes, and 20 were presumed nuclear explosions announced by ERDA. Of the last, 11 were at the Semipalatinsk test site, 2 at the Western Kazakh test site, 2 in Novaya Zemlya, 1 in the northern Urals, and the remaining 4 scattered across central Siberia. We thus have an unusually wide geographical distribution of explosion sources. All intermediate-depth earthquakes were located either in the Hindu Kush or Burmese seismic zones. Figure II-5 shows the locations of all the events studied, identified by X, Q, and D as explosion, shallow earthquake, and intermediate-depth earthquake, respectively.

For each event we have retrieved all the short-period (SP) detections, and 3-component long-period (LP) data, from each of the 9 Eurasian digital stations. The number of SP detections varied from 1 to 8 per event; no events were undetected. All the waveforms obtained were displayed and onset times picked on the SP data. Both body- and surface-wave magnitudes were determined where possible from each seismogram; here the automatic techniques described elsewhere in this SATS were of great use in reducing the amount of manual selection of amplitudes and periods required in magnitude determination. SP measurements were quite successfully made using these algorithms, and rarely needed to be reset. In the LP data, although few picks of peak 20-sec amplitude needed to be reset, a fairly high proportion (30 percent) had to be rejected as invalid, particularly for the smaller earthquakes and the explosions. Both Love-wave (after rotation of the 3-component data into radial and transverse components) and Rayleigh-wave measurements of  $M_g$  were made.

In a few cases, SP detections were made only at close (distance < 20°) stations and, in view of the general unreliability of  $m_b$  values made from such signals, the bulletin  $m_b$  was used instead of that determined from the station network used. The standard definitions of  $M_g$  and  $m_b$ , as used by the NEIS, and the Gutenberg-Richter distance-depth corrections for P amplitudes, were used throughout.

Figures II-6 and II-7 show  $M_g$  vs  $m_b$ , with  $M_g$  determined from Rayleigh and Love waves, respectively. The separation of shallow earthquakes (Q) from explosion (X) and intermediate-depth earthquake (D) populations is good down to  $m_b = 4.8$ , and better when  $M_g$  is determined from Love waves. The 11 shallow earthquakes of  $M_g < 3.5$  included: 3 in Iran, given bulletin depths > 45 km; 2 aftershocks of an earthquake in Kirgiziya; 1 in Tibet, and 1 in Mongolia for which clear depth phases indicated depths in excess of 15 km; and 4 in Szechwan, a region previously identified as one of anomalous  $M_g$ - $m_b$  values.<sup>3</sup>

We have also measured the discrimination parameters of complexity and spectral ratio, both of which are readily determined automatically once the P-wave onset time has been picked. The definitions used were those of Lacoss,<sup>4</sup> which he applied to LASA

$$\text{Complexity} = \frac{\sum_{t=P}^{t=P+5\text{sec}} S(t)}{\sum_{t=P+5\text{sec}}^{t=P+30\text{sec}} S(t)}$$

$$\text{Spectral Ratio} = \frac{\int_{1.56}^{2.03\text{Hz}} SP(f)}{\int_{0.39}^{0.94\text{Hz}} SP(f)}$$

where  $S(t)$  is the amplitude of the bandpass (0.6 to 3.0 Hz) filtered signal,  $P$  denotes signal onset time, and  $SP(f)$  is the amplitude spectrum of the waveform from  $t = P$  to  $t = (P + 10 \text{ sec})$ .

We tried modifying these definitions but obtained no discrimination improvement. Both discriminants proved to be extremely unreliable at distances of less than  $20^\circ$ , and were applied only to signals at distances greater than this. Some smaller events recorded only to short distances are thus excluded from the calculations. For both spectral ratio and complexity, the value obtained was an average over all stations used, and this proved to be a much better discriminant than individual values. The results obtained are shown in Figs. II-8 and II-9.

Network complexity values appear to be a surprisingly good discriminant, though it must be recalled that several smaller events have been rejected from the calculations for the reasons given above. Some of the apparently anomalous shallow earthquakes on the  $M_s$ - $m_b$  diagrams (Figs. II-6 and II-7) are, however, included in Fig. II-8 and good separation is obtained. Spectral ratio appears to be a poor discriminant. We plan to continue this study as more data become available. In addition, we hope to extend the current analysis to include the use of near (distance  $< 20^\circ$ ) SP data to determine  $m_b$ .

R. G. North

#### C. THE LIMITED RESEARCH VALUE OF THE SRO LONG-PERIOD RECORDS

To eliminate aliasing and to reduce microseismic noise, the LP digital channel of the SRO system includes a low-pass and 6-sec notch filter. The system originally deployed effectively removed from this channel all signal components above 0.1 Hz (see Fig. 5 in Ref. 5); consequently, the SP and LP pass bands do not overlap as they do, for example, in records from the WWSSN. The anti-alias filter was a 4-pole Butterworth with a corner at 0.1 Hz. This system is not sensitive to the weak onsets of the P-wave associated with propagation from near a node in the radiation pattern. Traditional fault-plane solutions depend on accurate reading of P-wave polarities and, in particular, on the polarities of the weaker signals.

A diminished sensitivity to first motions is illustrated with P-waves from a moderate-magnitude earthquake ( $M_g = 6.5$ ) that occurred on 18 November 1977 near the center of the Tibetan plateau. First motions have been read from the LP and SP records of the WWSSN. A comparison of records from CHG (Chang mai, Thailand) and ANP (Taiwan) with digital records from the corresponding SRO's CHTO and TATO [Figs. II-10(a) and II-11(a), and II-10(b) and II-11(b)] illustrate the disadvantage of the narrower pass band. The weak downward first motions are not recorded by the SRO system. The SP records confirm the onset times of the emergent first motion on the WWSSN LP records.

The effect of the anti-alias filter can be inferred from a comparison of analog SRO records [Figs. II-10(c) and II-11(c)] with the corresponding digital records. The analog record from CHTO shows a weak downward first motion similar to the first motion recorded by the WWSSN system. However, neither the analog nor the digital records from TATO recorded the downward first motion clearly seen on the corresponding WWSSN record. Apparently, the notch filter in the SRO system, by itself, accounts for a significant loss in high-frequency sensitivity.

Within the last year or so, the Butterworth anti-alias filter has been replaced by a less-dramatic Bessel filter (Gary Holcomb of the USGS Albuquerque Seismological Center has told us that near 0.167 Hz the new system response is down 11 dB from the peak magnification, whereas the old system is down 24 dB). However, because of the notch filter, the newer version of the SRO system still has a more narrow pass band than the WWSSN system. We would argue that



at least one channel from the SRO be made broad band, say the output from the seismometer sampled at 20 Hz. The microseisms can always be filtered out, if necessary, during processing. Harjes and Seidl<sup>6</sup> have also advocated broad-band recording based on data from the Graefenberg (GRF) broad-band seismic array.

T. J. Fitch  
M. W. Shields

#### REFERENCES

1. A. C. Strauss and L. C. Weltman, "Continuation of the Seismic Research Observatories Evaluation," Texas Instruments Report ALEX(01)-TR-77-02 (1977).
2. Seismic Discrimination Semiannual Technical Summary, Lincoln Laboratory, M.I.T. (30 September 1978), DDC AD-A065574/6.
3. T. E. Landers, "Some Interesting Central Asian Events on the  $M_s:m_b$  Diagram," Geophys. J. R. Astr. Soc. 31, 329-339 (1972).
4. R. T. Lacoss, "A Large-Population LASA Discrimination Experiment," Technical Note 1969-24, Lincoln Laboratory, M.I.T. (8 April 1969), DDC AD-687478.
5. D. W. McCowan and R. T. Lacoss, "Transfer Functions for the Seismic Research Observatory Seismograph System," Bull. Seismol. Soc. Am. 68, 501-512 (1978), DDC AD-A060931/3.
6. H. P. Harjes and D. Seidl, "Digital Recording and Analysis of Broad-Band Seismic Data at the Graefenberg (GRF)-Array," J. Geophys. 44, 511-523 (1978).

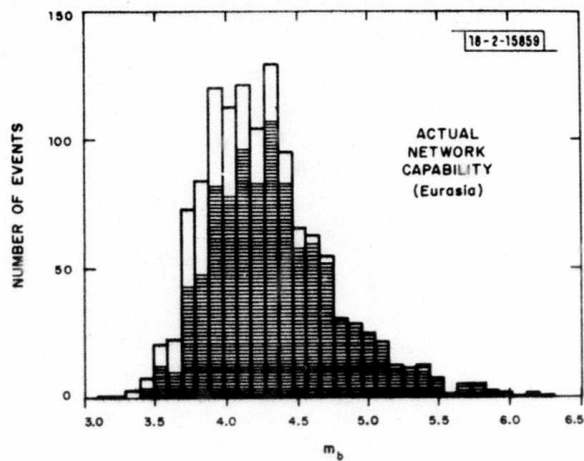


Fig. II-1. Detection performance of SRO/ASRO network, with respect to SDAC Bulletin time interval January to July 1978. Shaded portion designates detection by at least one station, white no detection. Events in Eurasia (here defined as northern half of eastern hemisphere) only used in evaluation here.

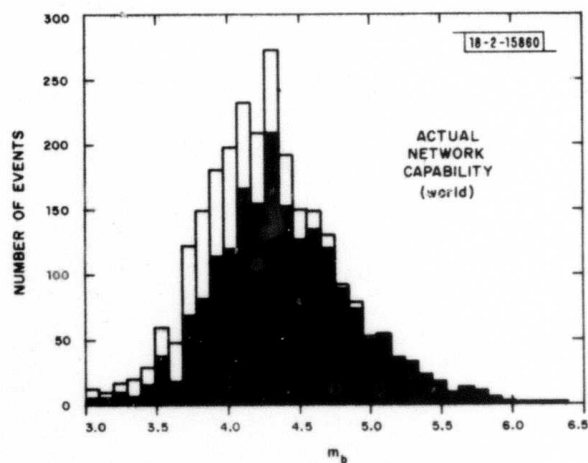


Fig. II-2. Same as for Fig. II-1, but for all events globally.

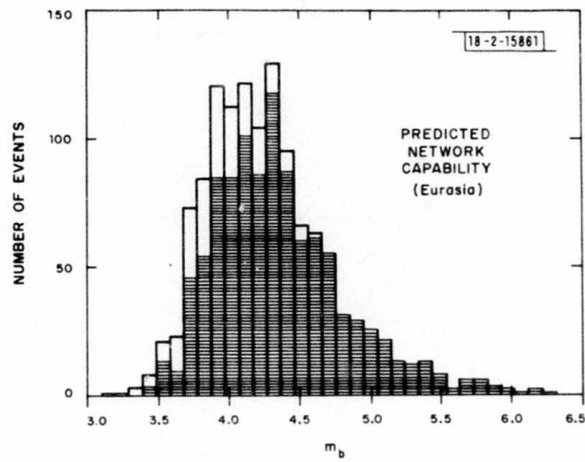


Fig. II-3. Predicted performance for Eurasia determined from observed individual station capability. See text for algorithm.

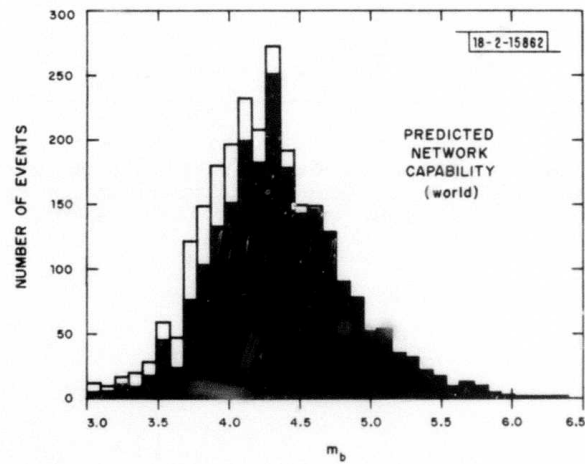


Fig. II-4. Same as for Fig. II-3, but for entire world.

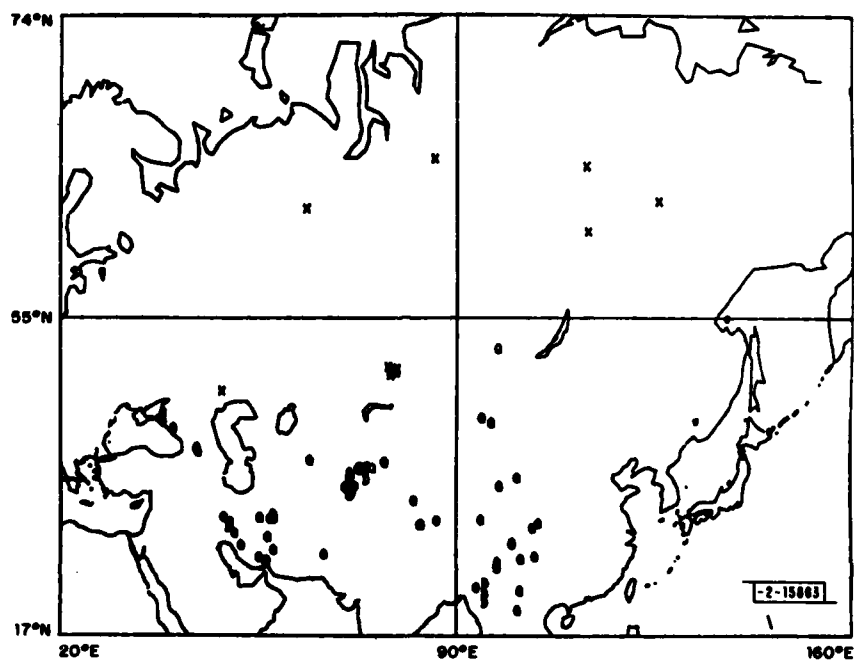


Fig. II-5. NEIS locations of events used in discrimination experiment. Presumed explosions, shallow earthquakes, and intermediate-depth earthquakes are denoted by X, Q, and D, respectively.

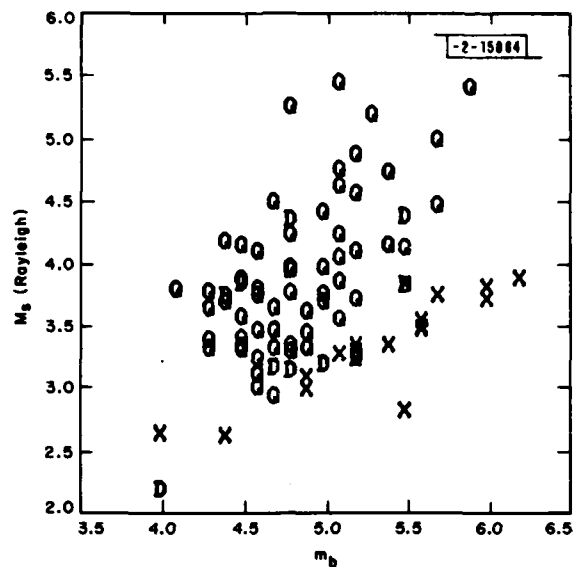


Fig. II-6. Values of  $M_s$  and  $m_b$  measured from SRO/ASRO digital data;  $M_s$  measured from Rayleigh-wave trains.

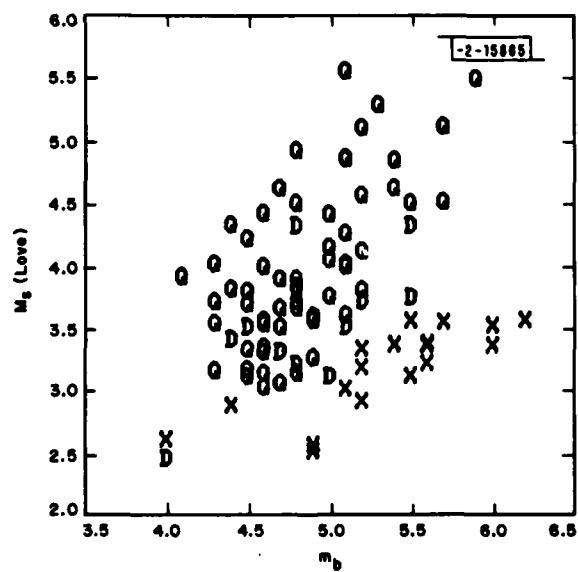


Fig. II-7. Same as Fig. II-6, but  $M_s$  measured from Love-wave trains.



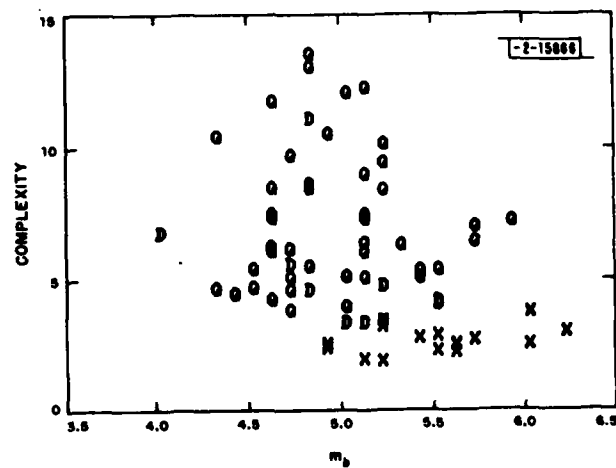


Fig. II-8. Measured values of complexity vs  $m_D$ .

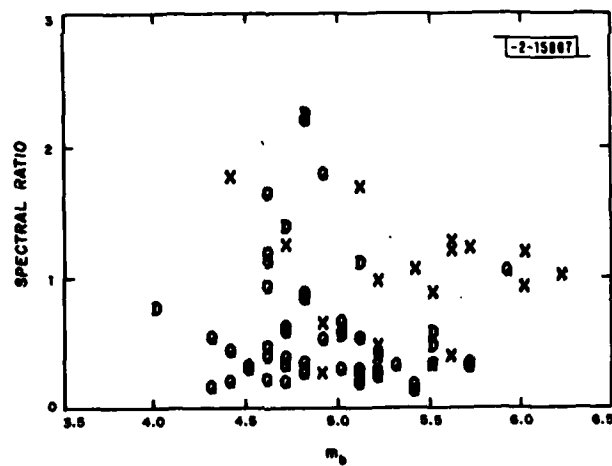


Fig. II-9. Measured values of spectral ratio vs  $m_D$ .

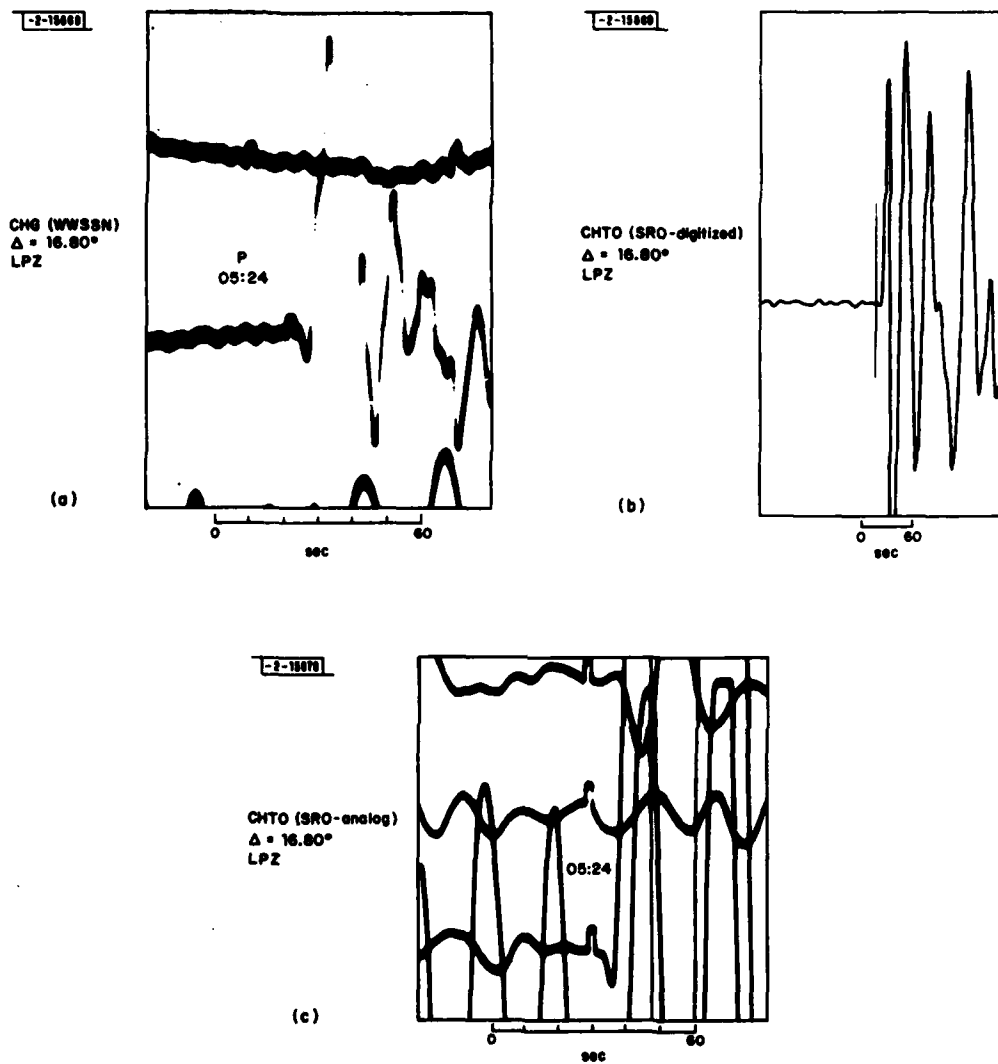


Fig. II-10. Long-period P-waves at Chang mai: vertical component (a) WWSSN, (b) SRO digital, and SRO analog.

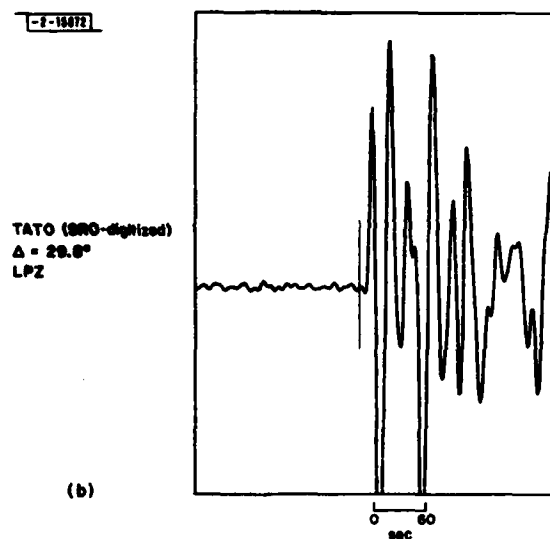
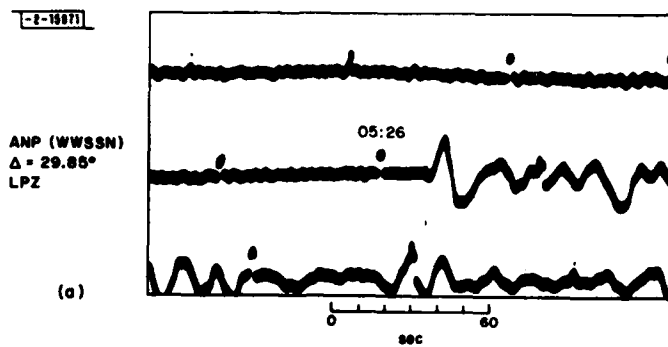


Fig. II-11. Long-period P-waves at Taiwan: vertical component  
 (a) WWSSN, (b) SRO digital, and (c) SRO analog.

[E-16873]

TATO (SRO-analog)  
 $\Delta = 29.8^\circ$   
LPZ

(c)



Fig. II-11. Continued.

### III. GENERAL SEISMOLOGY

#### A. SPECTRA OF CRUSTAL PHASES RECORDED DIGITALLY IN EASTERN CANADA

Spectra of Pn, Pg, and their S-wave equivalents have been computed from digital records from the Eastern Canada Telemetered Network (ECTN).<sup>1</sup> The records were supplied by W.E. Shannon of the Earth Physics Branch, Department of Energy, Mines and Resources, Ottawa. The vertical component of ground motions is sampled at 60 Hz by a recording system that is flat in velocity between 2 and 15 Hz. The spectra have been averaged and divided by  $\omega$  to simulate displacement spectra. The objectives of this project are to quantify the apparent anelastic properties of the lithosphere in eastern North America. From these preliminary results, it is clear that the shape of the spectra in the pass band from 2 to 15 Hz can fit functions of the form  $e^{-\alpha\omega}$  and  $\omega^{-\alpha}$  almost equally well. Also, the ratio of shear to compressional wave attenuation,  $Q\beta/Q\alpha$ , is close to unity. In contrast, this ratio is approximately 4 from teleseismic signals.<sup>2</sup>

Figure III-1 shows Pn and Sn spectra from an Arkansas earthquake ( $m_b = 4.9$ ) recorded at MIQ in southern Quebec. The epicentral distance is 1692 km. The difference in slopes implies a ratio of  $Q\beta/Q\alpha$  of approximately  $\sqrt{3}/2$ . Here it is assumed that the propagation medium is a Poisson's solid, and that the shaping of the spectra from source effects is the same for Pn and Sn in this pass band.

In Fig. III-2 are shown spectra for Pn and Pg recorded at GNT, a distance of 346 km from a small-magnitude earthquake that occurred in Maine on 18 April 1979. The spectra are nearly identical between 5 and 15 Hz; however, Pg is significantly richer in the lower-frequency energy, 2 to 5 Hz. This disparity suggests that the anelastic and/or scattering properties of the upper crust are significantly different from those of the lower crust and the sub-Moho lithosphere. The apparent velocity windows corresponding to these spectra are 7.06 to 6.29 km/sec for Pn, and 6.07 to 5.58 km/sec for Pg. Observations of frequency-dependent anelastic effects have also been reported by Aki and Chouet,<sup>3</sup> and by Aki.<sup>4</sup>

Finally, Fig. III-3 shows spectra of Pn and Sn from the Maine earthquake recorded at MNQ, a distance of 728 km from the epicenter. Both spectra have essentially the same shape; consequently, the ratio  $Q\beta/Q\alpha$  must be close to unity. To illustrate the similarity in the shapes of these spectra, a curve  $e(-\omega t^*/\pi)$  is shown where  $t^* = 0.1$ . Spectra of teleseismic P-waves from nuclear explosions yield  $t^*$ 's as low as 0.1 (see Ref. 5). The comparatively high Q of continental lithosphere demonstrated here and in a previous SATS<sup>6</sup> places constraints on the design of digital recording systems. Clearly, sampling rates and anti-alias filters must be chosen with the knowledge that high signal-to-noise ratios above 15 Hz are expected from small-magnitude earthquakes recorded at distances as great as 1000 km.

T. J. Fitch  
M. W. Shields

#### B. MORE MOMENT TENSOR ESTIMATION FROM LONG-PERIOD BODY WAVES

In a previous SATS,<sup>7</sup> a scheme for moment tensor estimation was tested with amplitude and first-motion data from body phases. The inversion mathematics are linear and therefore numerically efficient and free from uniqueness problems that plague many geophysical inverse problems. The inequalities that relate first-motion polarities to the moment tensor were represented



by asymmetric error functions of the L1 norm.<sup>8</sup> Asymmetric as well as symmetric error functions of this norm are shown in Fig. III-4. Minimization of the L1 norm yields solutions that are robust by comparison with solutions that minimize the L2 norm, the usual least-squares solution criterion.<sup>8,7</sup>

Here, we present solutions to three earthquakes of moderate magnitude for which the reduction of amplitudes to the focal sphere and the projection of ray paths have been varied by trial and error to maximize the double-couple (DC) component of the moment tensor. This experiment shows that within the realm of geophysical plausibility, earthquakes can be modeled by DCs - in these cases, point source DCs. This conclusion pertains to that part of the seismic spectrum represented by the LP body waves recorded in the teleseismic distance range.

Figure III-5 shows the DC component of the full moment tensor (solid curves) and the DC from a focal mechanism solution by Molnar and Sykes.<sup>9</sup> (In a previous SATS,<sup>7</sup> an incorrect comparison was presented. The near-source reflected phases, pP and sP, were misidentified. The correct identification of these phases from the LP records of the WWSSN is discussed in Fitch, McCowan, and Shields.<sup>10</sup>) The DC component was increased by 20 percent to 85 percent of the full moment tensor by systematically steepening the ray paths predicted for the direct and near-source reflected phases. This was achieved by assuming a source depth of 25 km in a Herrin earth, rather than sub-Moho depth appropriate for a depth of 25 km in oceanic lithosphere.

Figure III-6 shows a DC component that represents 71 percent of the full moment tensor for an earthquake at a mantle depth of 90 km beneath the Tibetan plateau.<sup>11</sup> In this case, the percentage DC was increased by 20 percent by assuming a near-surface compressional velocity of 5 km/sec instead of 6 km/sec. The lower velocity may be more representative of the near-surface rocks of the Tibetan plateau.

Figure III-7 shows a DC component for a deep-focus earthquake beneath the Bonin Island arc.<sup>10</sup> The data set includes P- and S-wave amplitudes recorded digitally by the SROs. This DC represents 78 percent of the moment tensor. A 20-percent enhancement of the DC component was achieved by reducing the compressional velocity assumed for the source region from the Herrin velocity of 9.11 km/sec to 8.64 km/sec, a 7-percent reduction. It should be emphasized that variations in the slope of the travel times to the different stations could manifest themselves as an apparent change in near-source velocity.

From these examples it is clear that, regardless of the mode of strain release, earthquakes of moderate magnitude can yield unconstrained moment tensors that are essentially pure DCs. In any case, the DC components are stable in that variations in the reduction of the amplitudes to the focal sphere and in the projection of the ray paths yield only minor differences in the DCs, say less than 10° in the angles that define the orientation of the nodal planes.

T. J. Fitch  
M. W. Shields

### C. SYNTHETIC SEISMOGRAMS FOR EXPLOSIVE SOURCES

Given a reduced velocity potential (RVP) function  $V(r)$ , the far-field radial displacement will be

$$u(r, t) = - \frac{V(t - r/\alpha)}{r} .$$

If, however, only the amplitude spectrum  $V(\omega)$  is known, then an additional assumption must be made to specify the phase spectrum. We have assumed that, of all the sampled waveforms

consistent with a given RVP amplitude spectrum, the observed one will be minimum phase. The minimum-phase condition has been widely discussed (e.g., Robinson<sup>12</sup>) and is equivalent to the statement that the energy in the resulting waveform be concentrated as much toward the beginning of the waveform as possible. This, we feel, is reasonable when the physics of the explosion process is considered.

Since our data consisted of log-log plots of the pertinent spectra, we interpolated them onto a linear frequency axis and then used Kolmogoroff's method<sup>13</sup> to do the spectral factorization. As an example, we show an observed RVP for the Salmon explosion observed 774 m away from ground zero in Fig. III-8, and the corresponding source time function in Fig. III-9. The time integral of this last figure is the explosive moment time history. We can see in Fig. III-9 that the energy is indeed scrunched up toward the beginning.

To produce realistic seismograms, a pP phase was added to the source with a reflection coefficient of 0.9 and delay time of 0.12 sec. The result was attenuated using a causal Q operator with a  $t^*$  of 0.5 and passed through the instrument response of the proposed NSS. The result is shown in Fig. III-10. The detail occurring after 1 sec in the waveform is due to the bumps and wiggles in Fig. III-8. Cube-root scaling and a pP delay time of 0.37 sec were used to produce the 150-kt version shown in Fig. III-11. Here the details in the waveform have been shifted up in frequency, where they were obliterated by attenuation. The result, therefore, looks very much like the attenuated instrument response for the NSS.

D. W. McCowan  
M. A. Tiberio

## REFERENCES

1. R. B. Hayman and W. E. Shannon, "Seismological Service of Canada: Instrumentation and Data Processing," *Phys. Earth Planet. Inter.* **18**, 95-104 (1979).
2. L. J. Burdick, " $t^*$  for S Waves with a Continental Ray Path," *Bull. Seismol. Soc. Am.* **68**, 1013-1030 (1978).
3. K. Aki and B. Chouet, "Origin of Coda Waves: Source, Attenuation and Scattering Effects," *J. Geophys. Res.* **80**, 3322-3342 (1975).
4. K. Aki, "Attenuation of Shear Waves in the Lithosphere for Frequencies from 0.5 to 25 Hz," to be published in the *Journal of Geophysical Research*.
5. Z. A. Der and T. W. McElfresh, "The Relationship between Anelastic Attenuation and Regional Amplitude Anomalies of Short-Period P-Waves in North America," *Bull. Seismol. Soc. Am.* **67**, 1303-1317 (1977).
6. Seismic Discrimination Semiannual Technical Summary, Lincoln Laboratory, M.I.T. (31 March 1979), DDC AD-A073772.
7. *Ibid.* (30 September 1978), DDC AD-A065574/6.
8. J. F. Claerbout and F. Muir, "Robust Modeling with Erratic Data," *Geophysics* **38**, 826-844 (1973).
9. P. Molnar and L. R. Sykes, "Tectonics of the Caribbean and Middle America Regions from Focal Mechanisms and Seismicity," *Geol. Soc. Am. Bull.* **80**, 1639-1684 (1969).
10. T. J. Fitch, D. W. McCowan, and M. W. Shields, "Estimation of the Seismic Moment Tensor from Teleseismic Body Wave Data with Applications to Intraplate and Mantle Earthquakes," to be published in the *Journal of Geophysical Research*.
11. W. P. Chen, T. J. Fitch, J. L. Nabeleh, and P. Molnar, "An Intermediate Depth Earthquake Beneath Tibet: Source Characteristics of the Event of September 14, 1976," *J. Geophys. Res.* (in press, 1979).
12. E. A. Robinson, *Multichannel Time Series Analysis with Digital Computer Programs* (Holden-Day, San Francisco, 1967).
13. J. F. Claerbout, *Fundamentals of Geophysical Data Processing* (McGraw-Hill, New York, 1976).

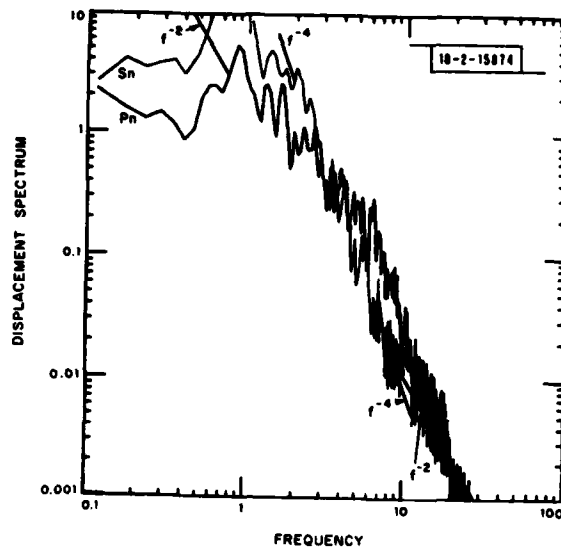


Fig. III-1. Relative displacement spectra for Pn and Sn at MIQ from Arkansas earthquake of 25 March 1976. Origin times: 00:41:20.5,  $m_b = 4.9$ . Also shown are lines illustrating spectral decays proportional to  $f^{-2}$  and  $f^{-4}$ .

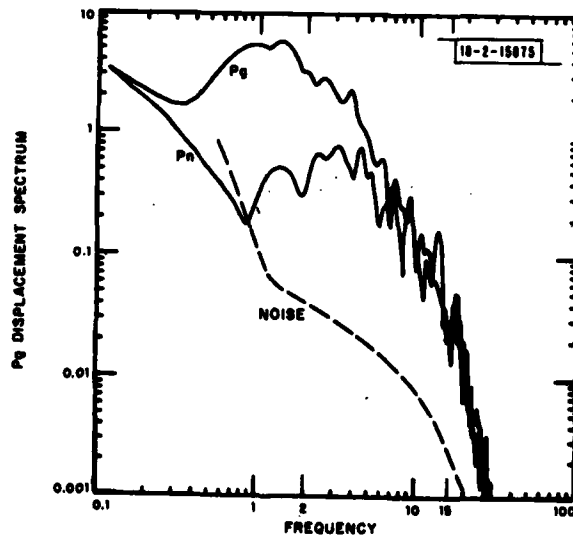


Fig. III-2. Relative displacement spectra for Pn and Pg at GNT from Maine earthquake of 18 April 1979. Spectrum of noise is sketched in as a dashed line.

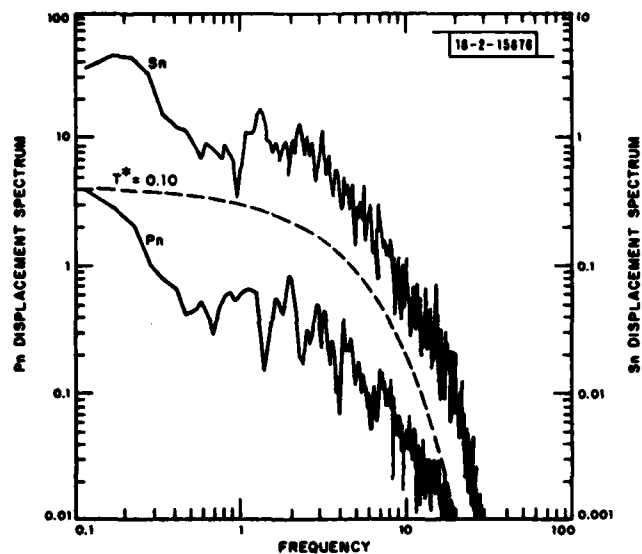


Fig. III-3. Relative displacement spectra of Pn and Sn at MNQ for Maine earthquake of 18 April 1979.

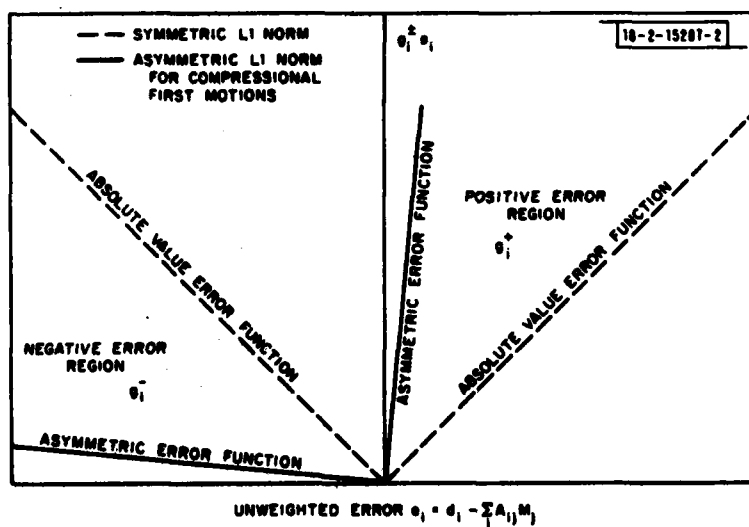


Fig. III-4. Asymmetric and symmetric error functions for L1 norm.

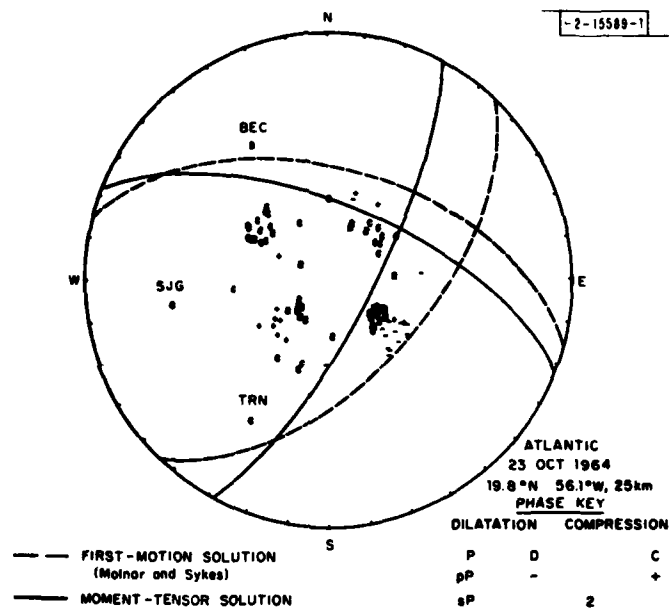


Fig. III-5. Comparison of DC from moment tensor inversion and first-motion study: equal-area projection of lower half of focal sphere.

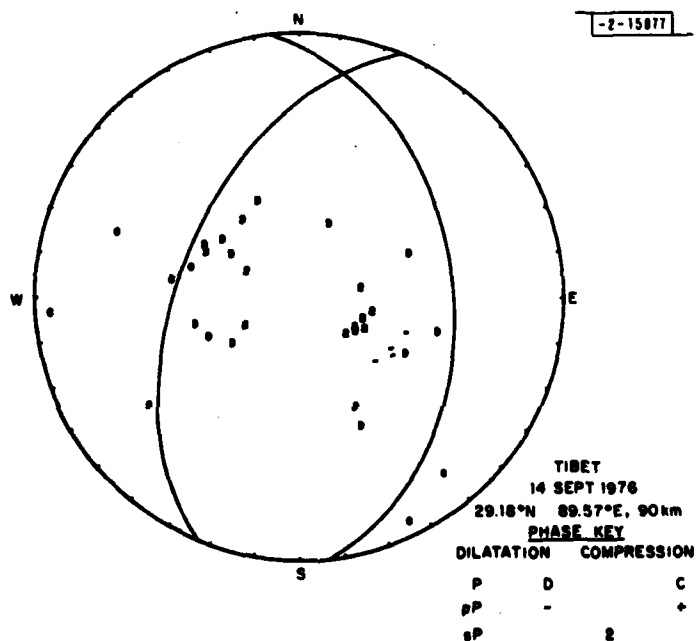


Fig. III-6. DC component from Tibetan earthquake: projection same as in Fig. III-5.

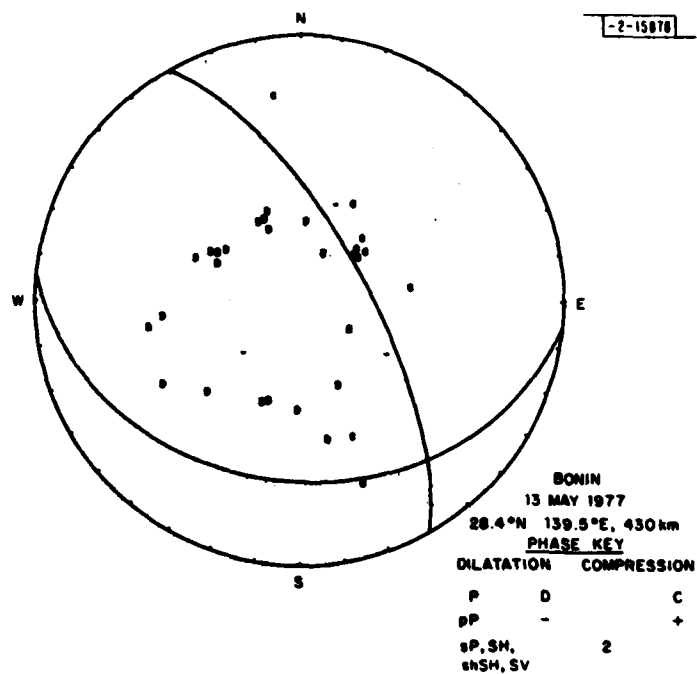


Fig. III-7. DC component from Bonin earthquake: projection same as in Fig. III-5.

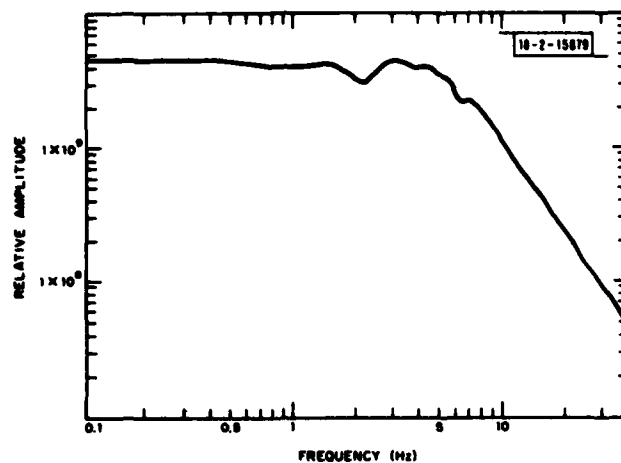


Fig. III-8. Salmon explosion reduced velocity potential amplitude spectrum for 5-kt yield, observed 774 m from ground zero.

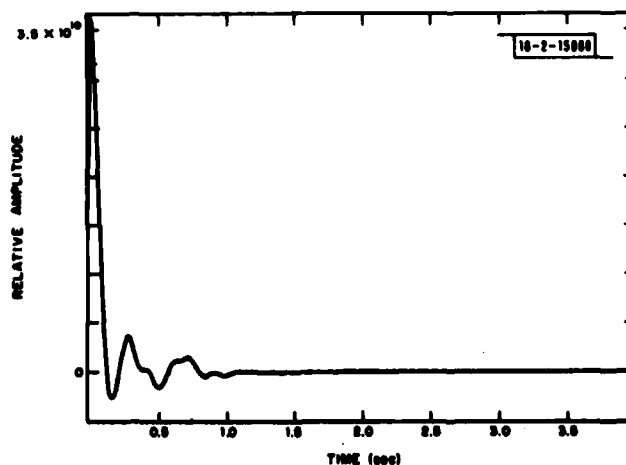


Fig. III-9. Source time function for Salmon explosion source with 5-kt yield.



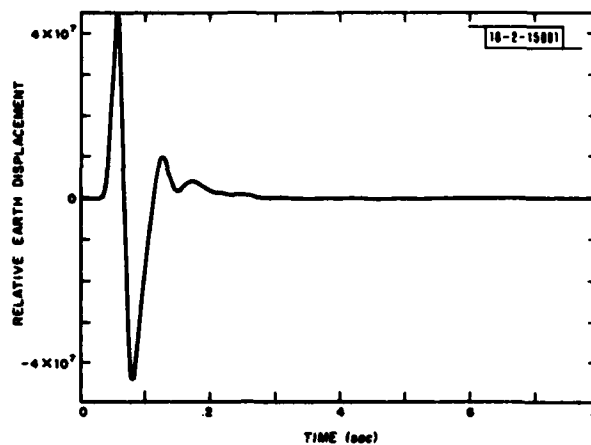


Fig. III-10. Salmon explosion synthetic seismogram for 5-kt yield. Attenuated with  $t^* = 0.5$ , pP reflection coefficient of 0.9, and delay time of 0.12 sec. Seen through NSS instrument response.

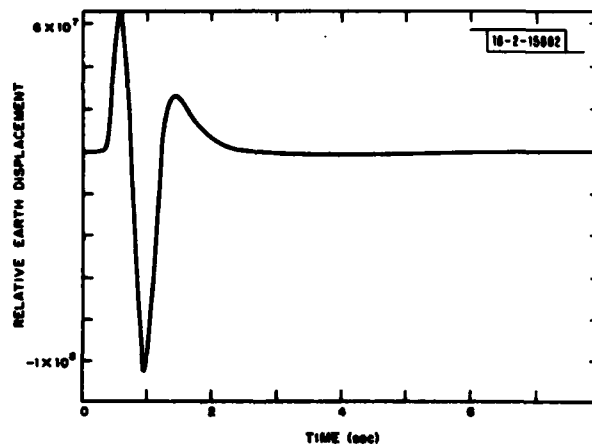


Fig. III-11. Same as Fig. III-10, but for 150-kt yield. Attenuated with  $t^* = 0.5$ , pP reflection coefficient of 0.9, and delay time of 0.37 sec. Seen through NSS instrument response.

#### IV. PUBLICATIONS LIST

The following list contains an update to the Seismic Discrimination Publications List printed in the 31 March 1977 SATS (DDC AD-A045453/8).

Requests for these reports or reprints should be addressed to:

The secretary  
Lincoln Laboratory Group 22  
42 Carleton Street  
Cambridge, MA 02142

167. Seismic Discrimination Semiannual Technical Summary, Lincoln Laboratory, M.I.T. (31 March 1977), DDC AD-A045453/8.
168. R. G. North, "Station Magnitude Bias - Its Determination, Causes, and Effects," Technical Note 1977-24, Lincoln Laboratory, M.I.T. (29 April 1977), DDC AD-A041643/8.
169. R. T. Lacoss, "Autoregressive and Maximum Likelihood Spectral Analysis Methods," NATO Advanced Study Institute Series, Aspects of Signal Processing, Part 2, G. Tacconi, Ed. (D. Reidel, Dordrecht-Holland, 1977), pp. 591-615, DDC AD-A050628/7.
170. D. W. McCowan and A. M. Dziewonski, "An Application of the Energy - Moment Tensor Relation to Estimation of Seismic Energy Radiated by Point and Line Sources," Geophys. J. R. Astr. Soc. 51, 531-544 (1977), DDC AD-A054403/1.
171. Seismic Discrimination Semiannual Technical Summary, Lincoln Laboratory, M.I.T. (30 September 1977), DDC AD-A050584/2.
172. C. W. Frasier and R. G. North, "Evidence for  $\omega$ -Cube Scaling from Amplitudes and Periods of the Rat Island Sequence (1965)," Bull. Seismol. Soc. Am. 68, 265-282 (1978), DDC AD-A060928/9.
173. D. K. Chowdhury and C. W. Frasier, "Evidence for Anisotropic Scattering of Short-Period P Phases in the Upper Mantle," Bull. Seismol. Soc. Am. 68, 609-618 (1978), DDC AD-A061205/1.
174. J. Berger, D. W. McCowan, W. E. Farrell, and R. T. Lacoss, Comments on "Transfer Functions for the Seismic Research Observatory Seismograph System," Bull. Seismol. Soc. Am. 68, 1537-1538 (1978).
175. Seismic Discrimination Semiannual Technical Summary, Lincoln Laboratory, M.I.T. (31 March 1978), DDC AD-A057279.
176. D. W. McCowan, "High-Resolution Group Velocity Analysis," Geoexploration 16, 97-109 (1978), DDC AD-A058020/9.
177. S. Seneff, "A Fast New Method for Frequency Filter Analysis of Surface Waves: Application in the West Pacific," Bull. Seismol. Soc. Am. 68, 1031-1048 (1978), DDC AD-A061212/7.
178. Seismic Discrimination Semiannual Technical Summary, Lincoln Laboratory, M.I.T. (30 September 1978), DDC AD-A065574/6.
179. J. D. Phillips and D. W. McCowan, "Ocean Bottom Seismometers for Research: A Reassessment," Technical Note 1978-40, Lincoln Laboratory, M.I.T. (30 November 1978), DDC AD-A064871/7.
180. D. W. McCowan, P. Glover, and S. S. Alexander, "A Crust and Upper Mantle Model for Novaya Zemlya from Rayleigh-Wave Dispersion Data," Bull. Seismol. Soc. Am. 68, 1651-1662 (1978), DDC AD-A069928.
181. D. W. McCowan and R. T. Lacoss, "Transfer Functions for the Seismic Research Observatory Seismograph System," Bull. Seismol. Soc. Am. 68, 501-512 (1978), DDC AD-A060931/3.
182. M. A. Chinnery, "Measurement of  $m_b$  with a Global Network," Tectonophysics 49, 139-144 (1978), DDC AD-A065031/7.
183. Seismic Discrimination Semiannual Technical Summary, Lincoln Laboratory, M.I.T. (31 March 1979), DDC AD-A073772.

184. J. A. Fitch, "Earthquakes and Plate Tectonics," in The Earth: Its Origin, Structure and Evolution (Academic Press, London, 1979), pp. 491-542.
185. M. A. Chinnery, "A Comparison of the Seismicity of Three Regions of the Eastern U.S.," Bull. Seismol. Soc. Am. 69, 757-772 (1979).
186. J. A. Jackson and T. J. Fitch, "Seismotectonic Implications of Relocated Aftershock Sequences in Iran and Turkey: An Application of the Master Event Technique," Geophys. J. R. Astr. Soc. 57, 209-229 (1979).

## GLOSSARY

AFTAC	Air Force Tactical Applications Center
ASRO	Abbreviated Seismic Research Observatory
DARPA	Defense Advanced Research Projects Agency
ECTN	Eastern Canada Telemetered Network
ERDA	Energy Research and Development Agency
ISC	International Seismological Center
LASA	Large-Aperture Seismic Array
NEIS	National Earthquake Information Service
NSS	National Seismic Station
PDE	Preliminary Determination of Epicenter
SATS	Semiannual Technical Summary
SDAC	Seismic Data Analysis Center, Alexandria, VA
SDC	Seismic Data Center
SDMS	Seismic Data Management System
SRO	Seismic Research Observatory
USGS	U.S. Geological Survey
WMO/GTS	World Meteorological Organization's Global Telecommunication System
WWSSN	World-Wide Standard Seismograph Network

UNCLASSIFIED

SECURITY CLASSIFICATION OF THIS PAGE (When Data Entered)

19 REPORT DOCUMENTATION PAGE		READ INSTRUCTIONS BEFORE COMPLETING FORM
1. REPORT NUMBER 18 ESD-TR-79-247 ✓	2. GOVT ACCESSION NO.	3. RECIPIENT'S CATALOG NUMBER
4. TITLE (and Subtitle) 6 Seismic Discrimination A073 772	5. TYPE OF REPORT & PERIOD COVERED 9 Semiannual Technical Summary rept. 1 Apr - 30 Sep 1979	
7. AUTHOR(s) 10 Michael A. Chinnery	6. PERFORMING ORG. REPORT NUMBER	
9. PERFORMING ORGANIZATION NAME AND ADDRESS Lincoln Laboratory, M.I.T. P.O. Box 73 Lexington, MA 02173	8. CONTRACT OR GRANT NUMBER(s) 15 F19628-78-C-0002 ✓ ARPA Order-512	
11. CONTROLLING OFFICE NAME AND ADDRESS Defense Advanced Research Projects Agency 1400 Wilson Boulevard Arlington, VA 22209	10. PROGRAM ELEMENT, PROJECT, TASK AREA & WORK UNIT NUMBERS ARPA Order 512 Program Element No. 62701E Project No. 9F10	
14. MONITORING AGENCY NAME & ADDRESS (if different from Controlling Office) Electronic Systems Division Hanscom AFB Bedford, MA 01731	13. NUMBER OF PAGES 44 1240	
16. DISTRIBUTION STATEMENT (of this Report) Approved for public release; distribution unlimited.	15. SECURITY CLASS. (of this report) Unclassified	
17. DISTRIBUTION STATEMENT (of the abstract entered in Block 20, if different from Report)		
18. SUPPLEMENTARY NOTES None		
19. KEY WORDS (Continue on reverse side if necessary and identify by block number) seismic discrimination      surface waves      NORSAR seismic array      body waves      ARPANET seismology      LASA		
20. ABSTRACT (Continue on reverse side if necessary and identify by block number) Lincoln Laboratory is continuing the task of carrying out the design and specification of a Seismic Data Center which will fulfill U.S. obligations that may be incurred under a possible future Comprehensive Test Ban Treaty. This report includes 9 contributions, summarizing progress in the Data Center design and associated seismic research. These contributions are grouped as follows: Seismic Data Center (3 studies), analysis of Seismic Research Observatory data (3 studies), and general seismology (3 studies). An update to the Publications List is included.		

UNCLASSIFIED

SECURITY CLASSIFICATION OF THIS PAGE (When Data Entered)

207650

JOB